



Article

Numerical Investigation of a Foundation Pit Supported by a Composite Soil Nailing Structure

Wei Han ^{1,2,†} , Genxiao Li ^{3,†}, Zhaohui Sun ³, Hengjie Luan ^{1,*}, Chuanzheng Liu ⁴  and Xianlong Wu ³

¹ State Key Laboratory of Mining Disaster Prevention and Control Co-Founded by Shandong Province and the Ministry of Science and Technology, Shandong University of Science and Technology, Qingdao 266590, China; sdkdhwei@163.com

² Graduate School of Engineering, Nagasaki University, Nagasaki 852-8521, Japan

³ Shandong Provincial Key Laboratory of Civil Engineering Disaster Prevention and Mitigation, Shandong University of Science and Technology, Qingdao 266590, China; ligenxiao7983@163.com (G.L.); sdustrsh@163.com (Z.S.); sdust_wxl@163.com (X.W.)

⁴ School of Environment and Resource, Southwest University of Science and Technology, Mianyang 621000, China; lcuanzeng@yeah.net

* Correspondence: luanjie0330@126.com; Tel.: +86-176-6095-7080

† These authors contributed work equally and should be regarded as co-first authors.

Received: 2 January 2020; Accepted: 3 February 2020; Published: 6 February 2020



Abstract: In special geology conditions such as silt-soil, foundation pits are prone to instability and severe deformation. In this paper, a composite soil nailing structure was studied and its effect on a silt-soil symmetrical foundation pit investigated. The factors affecting the stability of the pit as well as its deformation characteristics were also explored. The results show that excavation depth of the foundation pit has a significant impact on its stability. The soil outside the foundation pit is in the form of a parabola, and the uplift of the soil mainly occurs at the bottom. The horizontal displacement of soil on the side wall of the foundation pit presents a “bulk belly” form. In addition, the axial force of soil nails is larger in the middle part, and smaller at both ends in the shape of a spindle. Moreover, the horizontal displacement is positively correlated with the inclination and spacing of the soil nails, but negatively correlated with the diameter and depth of the mixing pile inlay. Furthermore, the inclination and spacing of the soil nails, the diameter, and embedded depth of the mixing pile have their own critical values for stability of the foundation pit. Specifically, in this paper, with respect to soil nails, inclination should be below 30° and prestress value should not exceed 20 kN. With respect to the mixing pile, the diameter should be less than 1.5 m; when the embedded depth of the mixing pile exceeds the critical depth, the limiting effect of the mixing pile on horizontal displacement is not significant. This research provides important takeaways for the design of a composite soil nailing structure for symmetrical foundation pits.

Keywords: silt-soil soil; symmetrical foundation pit; composite soil nailing; mixing pile

1. Introduction

The eastern coastal areas of China are home to silt and soft soil, which has high moisture content, low density, high compressibility, and low bearing capacity, and, as a result, is prone to collapse and support failure. Although soil nailing structures have been developed extensively since the 1970s, they have limited applications in soft soil. In order to broaden the application range, a composite soil nailing structure was proposed. This paper studies the factors affecting the stability of a silt-soil symmetrical foundation pit and deformation characteristics of composite soil nailing.

At present, model experiments and theoretical research have been focusing on mixing pile composite soil nailing support [1–5]. Several construction cases have confirmed that a mixing pile can improve bearing capacity, minimize lateral movement, reduce total and differential settlement, and increase slope stability [6–8]. Lin et al. [9] used Midas to analyze the mechanical behavior of soil nails in a foundation pit with the support of mixed pile composite soil nailing, considering that the arrangement of prestressed soil nail can be concentrated in favor of soil nails in the upper layer. Huang et al. [10] demonstrated that the advanced micro-pile composite soil nailing support and walls of a foundation pit form an integrated structure and combination effect, which can effectively control soil deformation, and significantly reduce the tensile area and settlement of the slope. Zeng et al. [11] simulated a soft soil slope with the support of a soil nailing structure, and reported that high-pressure grouting can significantly prevent the occurrence of ground subsidence and deformation and that the soil-shaped “juzube nucleus” force distribution is affected by factors such as depth of the foundation pit excavation and action time. Yu and Zou [12] conducted soil slope model tests to analyze the behavior of soil when different load levels are added to the top of the slope (eventually resulting in soil slope damage), and analyzed influence factors such as nail length, inclination, distribution density, and soil density. Zhang et al. [13] and Guo et al. [14] considered the construction characteristics of a soil nailing structure, and discussed the influence of soil layer and soil nail layout on the axial force and displacement of soil nails. Zeng [15] introduced composite soil nailing support technology from two aspects: the main structural form and the main principle. He believed that advanced micro-piles with pre-stress anchors have a significant effect on slope stability. Xu [16] established a finite element model of soil nail mixing piles and compared it with pure soil nail support systems under the same conditions. The author concluded that horizontal and vertical deformation of the mixing pile was a result of its own strength and the strong friction of the soil against the pile, which controls overall deformation. Lin [17] believed that horizontal deformation of the composite soil nail wall had a “broom” shape, similar to the cantilever structure in the early stage of excavation. In the middle and later stages, the stiffness of soil nails plays a major controlling role as deformation gradually increases. Huang et al. [18] found that the surface of the soil nailing structure restricts deformation, the lateral pressure of the soil is transmitted to the soil nails, and the axial force between adjacent soil nails is adjusted. Hui et al. [19] indicated that excavation and exposure time without brackets should be strictly controlled during construction. Yu [20] investigated the design and detection of support structures for soft soil foundation pits alongside highways. They found that foundation pit excavation had creep characteristics. With excavation of each layer of soil, the settlement rate was found to move from large to small. The final settlement value was found to be large, but a support effect was not discussed in the study.

Most of the papers outlined above discuss the mechanical behavior of composite soil nailing structures with a mixing pile and their support mechanisms for foundation pits. However, research on composite soil nailing support and deformation characteristics of the support system in complex geological conditions is rare. In this paper, the influence degree of factors affecting the displacement of a symmetrical foundation pit were analyzed based on an orthogonal test. Subsequently, the displacement and axial force at several points in the foundation pit were studied. Finally, support structure parameter analysis for the displacement was conducted.

2. Project Overview

2.1. Background

The location of this project is an area west of the Qingdao tunnel hub (Figure 1a). Seven residential buildings with 18–26 floors are proposed to be built here. The foundation pit of the construction site offers temporary support. Ground elevation around the foundation pit is 5.6–7.0 m, supported after uniform excavation to a height of 6.0 m. Except for surface backfilling, the soil layer is silty clay. The soil has lower shear strength, larger porosity and rheological properties, and higher water content and sensitivity. The excavation of this soil layer has a great influence on the stability of the wall and the

surrounding soil. Therefore, deformation at the top of the foundation pit was monitored; distribution of the monitoring points outside the foundation pit is shown in Figure 1b. L10~L20 denote the first row of monitoring points, L36~L46 the second, and L61~L71 the third. Site selection for the measuring points was not done at random. Previous monitoring experience in the Qingdao area [21] revealed the following: deformation of foundation pits is mainly found in the vertical direction, the largest rheological deformation is on the bottom of the pit, and horizontal deformation mainly occurs on the side wall. The influence of soil deformation is about twice the depth of the foundation pit. Maximum vertical deformation of the soil is $0.7 H \sim 1.0 H$ behind the wall (H is excavation depth). Therefore, the monitoring range should be within 20 m from the sidelines of the foundation pit, and the monitoring points should be within the deformation range. A large sample of monitoring points is presented in Figure 1c.

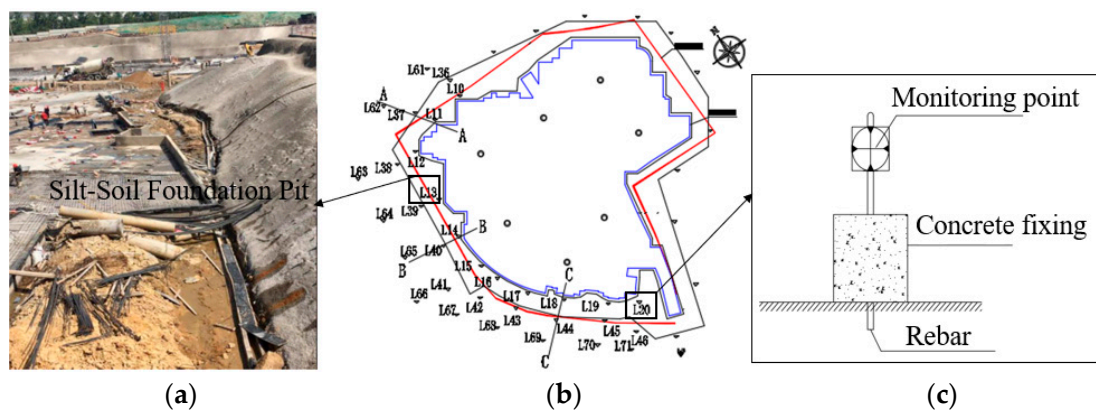


Figure 1. Location of the Silt-Soil Foundation Pit at Qingdao: (a) Mixing pile composite soil nail support project; (b) Distribution of the monitoring points; (c) Large sample of monitoring points.

2.2. In Field Monitoring

2.2.1. Horizontal Displacement

The horizontal displacement at the top of the foundation pit is presented in Figure 2a. As the distance from the foundation pit increases, the horizontal displacement at the top of the slope gradually decreases. Therefore, displacement at the top of the foundation pit should be keenly monitored during the construction process. Here, maximum horizontal displacement at the top of the foundation pit was monitored at 20.23 mm, as the monitoring alarm value was 30 mm. It is feasible to control the horizontal displacement at the top of the foundation pit when it is between 0.3% and 0.5% of pit depth. The results show that the maximum horizontal displacement of the foundation pit did not exceed 40 mm, and the monitoring results met construction requirements.

2.2.2. Vertical Settlement

The settlement curve at the top of the foundation pit is shown in Figure 2b. The maximum value occurs at a position about 6 m from the edge of the pit. The settlement value in the middle of the side wall is relatively large, while that in the corner is relatively small. Therefore, the central position in the side wall should be monitored. The maximum settlement value was found to be 17.64 mm. The maximum value of ground subsidence monitoring was found to be 30 mm, and the monitoring results met construction monitoring requirements.

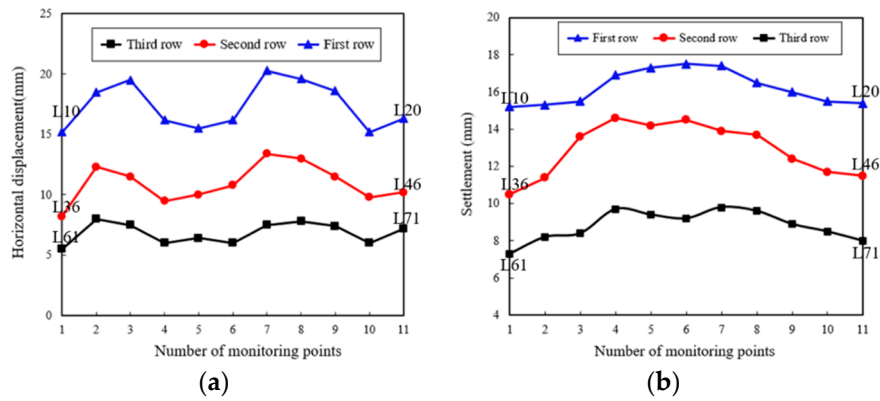


Figure 2. Foundation pit monitoring results: (a) Monitoring chart for horizontal displacement; (b) Monitoring chart for slope settlement.

3. Factors Affecting Stability

3.1. Numerical Model

In this paper, numerical modeling software FLAC3D was used to analyze the deformation and stability of a symmetrical foundation pit that was supported by a composite soil nailing structure. The calculation model and boundary conditions are presented in Figure 3. In the numerical model, a cable element was chosen for soil nailing and a solid element for the foundation pit. The upper surface was identified as a stress boundary. The vertical and horizontal displacements, as well as angles of rotation, were fixed to the base, so the bottom surface boundary was found to be fixed bearing support. As there is no restraining effect on the four side boundaries of the model in a vertical direction, horizontal displacement was constrained; thus, the boundary condition was identified as slip bearing support. The load conditions include additional top surface loads (0.02 MPa in this situation) and soil pressure. Groundwater pressure was not taken into consideration because an agitated pile water-proof curtain was embedded in the impervious layer of the foundation pit before excavation, and elevation of groundwater level dropped to below the basement surface. It should also be noted that the Mohr-Coulomb model was selected to describe stress-strain behavior in the numerical model. Through a geological survey of soil, pull-out experiment on soil nails, and mechanical laboratory tests on mixing piles, we were able to obtain the parameters of the corresponding materials; they are shown in Tables 1–3.

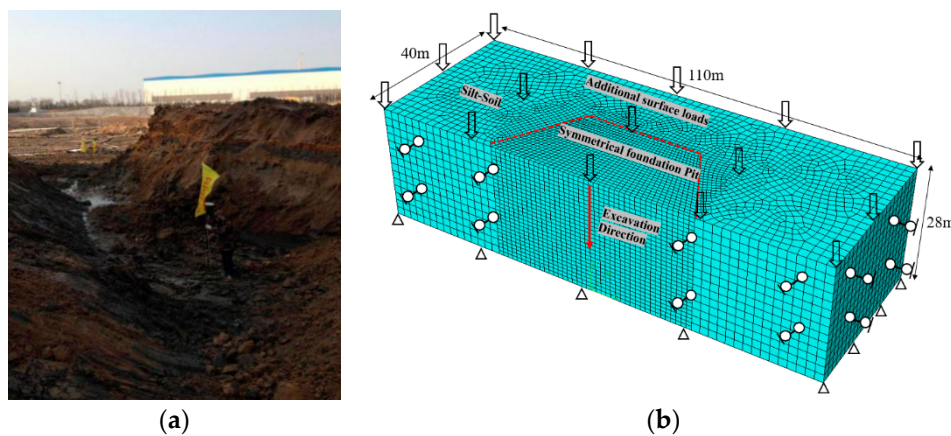


Figure 3. Calculation model used in this paper: (a) Site pit map; (b) Symmetrical computational model.

Table 1. Parameters of soil.

Parameters	Value
Elastic Modulus/(MPa)	18
Poisson's ratio	0.3
Cohesion/(kPa)	18
Internal friction angle/(°)	20
Natural severe (kN/m ³)	18.5

Table 2. Parameters of mixing piles.

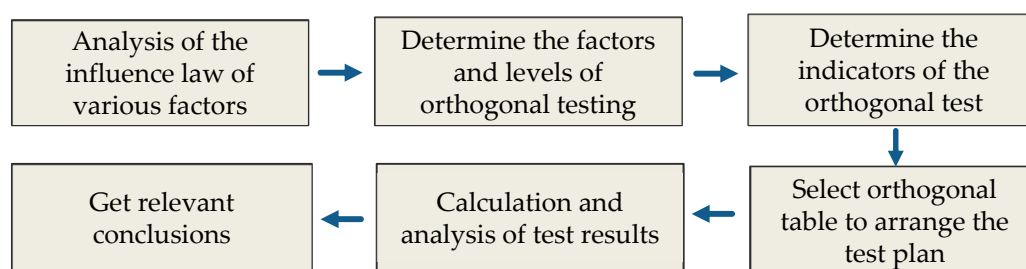
Parameters	Value
Unconfined compressive strength/(MPa)	1
Cohesion/(kPa)	200
Deformation modulus/(MPa)	120
Internal friction angle/(°)	20
Poisson's ratio	0.3
Bulk modulus/(MPa)	100
Shear modulus/(MPa)	46.15

Table 3. Parameters of soil nailing.

Parameters	Value
Elastic modulus/(MPa)	2.4×10^4
Tensile strength/(MPa)	30
Poisson's ratio	0.25
Cross-sectional area (mm ²)	314.2
Thermal expansion coefficient	0

3.2. Orthogonal Test

In order to identify the factors affecting the stability of a silt-soil foundation pit supported by composite soil nailing, the orthogonal test was conducted. The test, which has three main design factors—indicators, factors, and levels—has long been used to investigate multi-influence factor optimization experiments. The main steps are shown in Figure 4.

**Figure 4.** Orthogonal test steps.

3.3. Design of the Orthogonal Test

In this paper, five control indicators were selected and four levels of influence were chosen for each influencing factor, as per the actual project. Numerical simulation test was conducted by the $L_{16}(4^5)$ orthogonal table. It should be noted that 16, 4, and 5 represent the number of tests, levels, and control indicators, respectively. The five control indicators are surface settlement S_1 , horizontal displacement D of the foundation pit, maximum shear stress T of the soil, axial force N of the soil nail, and uneven settlement S_2 of the surrounding foundation pit. The five influencing factors include excavation depth h , horizontal distance H of the building around the foundation pit from its edge,

elastic modulus E , cohesive force C , and internal friction angle φ of the soil layer. The five factors of the orthogonal test were selected at four levels for testing. With respect to h , four levels of 4 m, 8 m, 12 m, and 16 m were selected. For H , 3 m, 6 m, 9 m, and 12 m were chosen. In addition, the four levels for the influencing factors E , C , and φ are listed in Table 4. Table 5 shows the values of the orthogonal experiment design, which are based on a combination of levels shown in Table 4.

Table 4. Serial number of each factor level and its value.

Level	h (m)	H (m)	E (MPa)	C (kPa)	φ (°)
1	4	3	6	5	10
2	8	6	9	15	15
3	12	9	12	35	27
4	16	12	15	55	45

Table 5. Orthogonal experiment design values.

Number	h (m)	H (m)	E (MPa)	C (kPa)	φ (°)
1	(1)4	(1)3	(1)6	(1)5	(1)10
2	(1)4	(2)6	(2)9	(2)15	(2)15
3	(1)4	(3)9	(3)12	(3)35	(3)27
4	(1)4	(4)12	(4)15	(4)55	(4)45
5	(2)8	(1)3	(2)9	(2)15	(4)45
6	(2)8	(2)6	(1)6	(4)55	(3)27
7	(2)8	(3)9	(4)15	(1)5	(2)15
8	(2)8	(4)12	(3)12	(3)35	(1)10
9	(3)12	(1)3	(3)12	(4)55	(2)15
10	(3)12	(2)6	(4)15	(3)35	(1)10
11	(3)12	(3)9	(1)6	(2)15	(4)45
12	(3)12	(4)12	(2)9	(1)5	(3)27
13	(4)16	(1)3	(4)15	(2)15	(3)27
14	(4)16	(2)6	(3)12	(1)5	(4)45
15	(4)16	(3)9	(2)9	(4)55	(1)10
16	(4)16	(4)12	(1)6	(3)35	(2)15
\overline{T}_{ij}	T_{ij} is the sum of the test indicator values for all factor i and level j				
\overline{T}_{ij}	$\overline{T}_{ij} = T_{ij}/4$				
R	$R = \max(\overline{T}_{ij}) - \min(\overline{T}_{ij})$				

3.4. Orthogonal Test Results

In this paper, the simulation results of each control indicator are calculated by range analysis formula, and the calculated value of R is plotted into a curve. The analyses are shown below. As shown in Figure 5a, the degree of influence on surface settlement around the excavated foundation pit is $h > E > H > C > \varphi$; the degree of influence on horizontal displacement of the foundation pit is shown in Figure 5b, which is $h > E > \varphi > H > C$. For indicator N , the degree of influence for soil nail maximum axial force is $h > \varphi > C > E > H$. For indicator T , the degree of influence for maximum shear stress of the surrounding soil is $h > C > E > H > \varphi$. As the results show, excavation depth h of the foundation pit is the most important factor for stability of the composite soil nail support. When excavation depth h increases, the five control indicators show an upward trend.

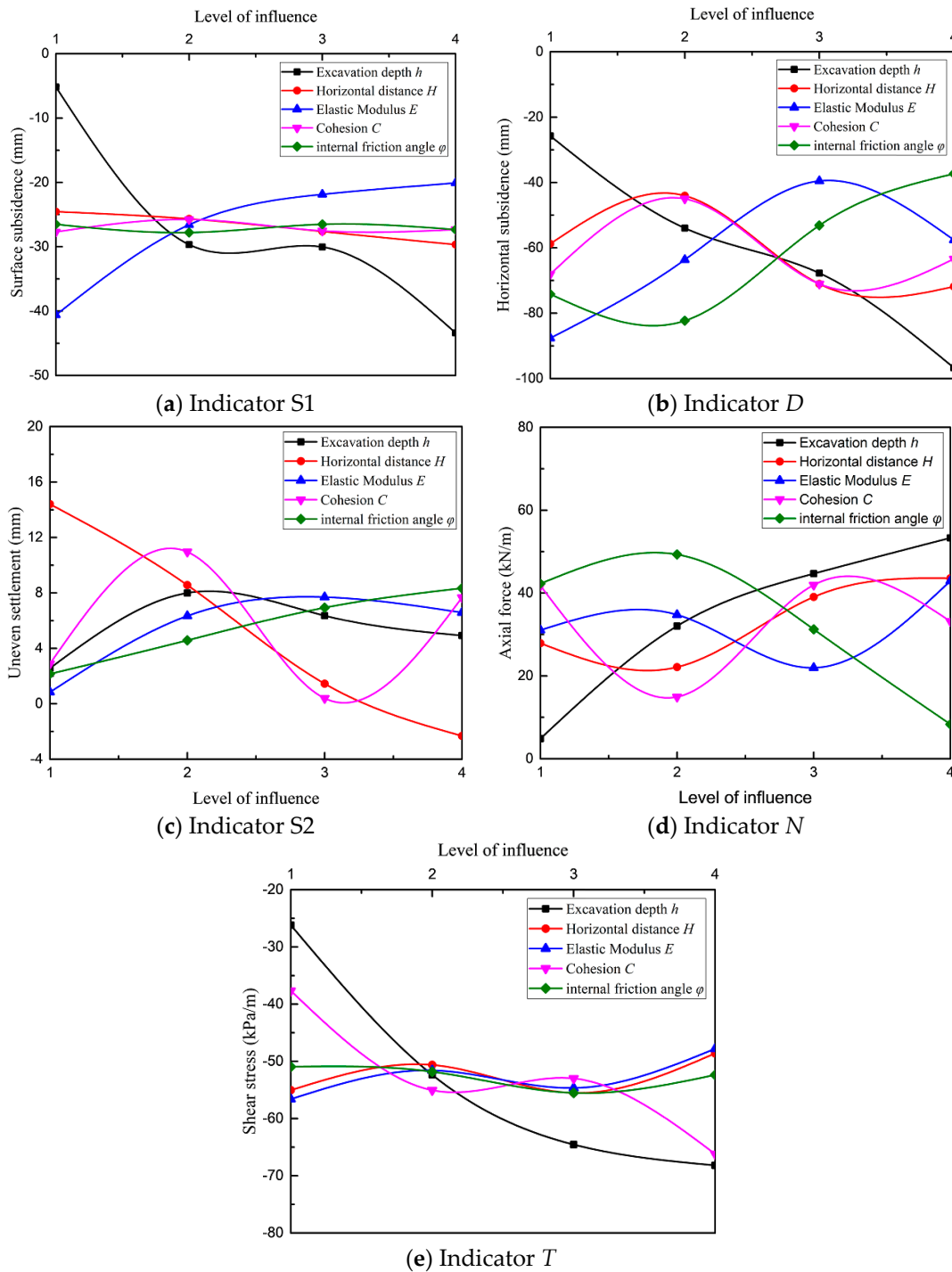


Figure 5. Mean value of the control indicators and changes in curve level.

The distance H between the building and the excavation boundary of the foundation pit has a relatively small influence on the five control indicators. This is mainly related to the construction method selected for the foundation pit and the support structure. However, when distance H is small, the load on the side of the foundation pit after excavation makes the slope unstable and the sliding force further increases; this can cause slope damage. In addition, in indicator S2, the degree of influence on uneven settlement of surrounding buildings is $H > C > E > \phi > h$. Distance H from the excavation edge of the foundation pit is the largest factor influencing the control indicator. It indicates that the distance

between the foundation and the surrounding buildings should be reasonably controlled during the construction of the foundation pit in order to avoid uneven settlement of the surrounding buildings.

For indicator T , the value of C and φ play a key role in judging the failure state of soil in the numerical simulation. Except for depth (h) and elastic modulus E , the values of C and φ (25.8% and 13%, respectively) are factors greatly affecting the excavation of the foundation pit. When excavation depth (h) of the foundation pit is constant, soil pressure behind the wall decreases gradually as the value of C and φ increases.

Overall, the primary and secondary order of stability of the foundation pit supported by composite soil nailing of the mixing pile in muddy soft soil is affected by various influencing factors: $h > E > C > \varphi > H$.

4. Numerical Results

4.1. Vertical Displacement

Figure 6 presents the settlement of soil inside and outside the foundation pit. Maximum settlement occurs about 5 m from the edge of the pit, settlement value is 15.05 mm, and maximum settlement value of on-site monitoring is 17.64 mm. There is about 10 mm settlement at 20 m from the edge of the pit, which indicates that the composite soil nail support has poor control on the settlement outside the pit. With simulation, it is not difficult to identify the settlement value of the soil outside the foundation pit. The distance from the edge of the foundation pit is in the form of a parabola. This is because when excavation depth is shallow, the influence of excavation on rebound deformation of the soil outside the foundation pit is far greater than that caused by the horizontal displacement of soil on the side wall, making the vertical displacement of soil outside the foundation pit appear as a bulge. On the contrary, when excavation depth is deep, the horizontal displacement of the side wall increases with rise in excavation depth, and its influence on soil outside the foundation pit exceeds the rebound deformation of the soil generated by excavation unloading. This causes the vertical displacement of soil outside the pit to look like a settlement.

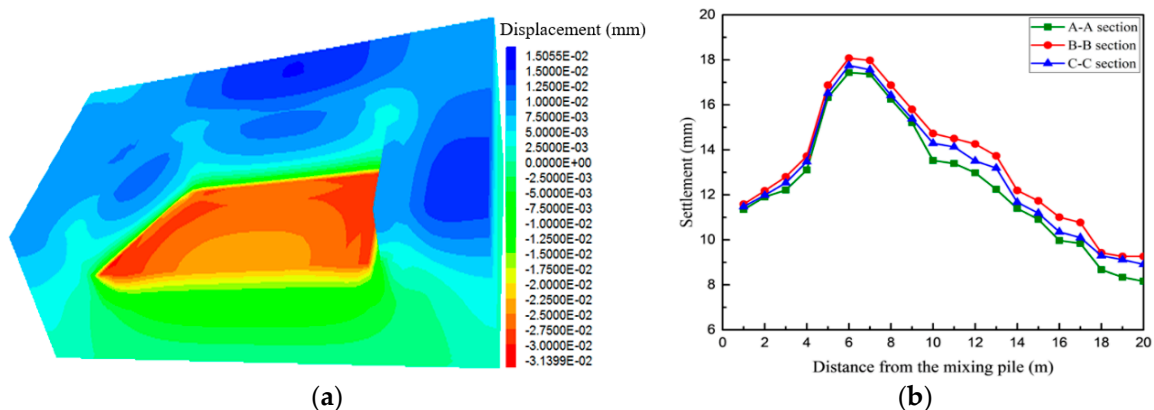


Figure 6. Settlement of soil inside and outside the foundation pit: (a) Cloud diagram of soil settlement in the foundation pit; (b) Monitoring curve for the foundation pit settlement.

It can be seen from Figure 6a that soil uplift mainly occurs in the bottom of the pit. As per the variation law, the uplift value at the bottom edge of the pit is larger and that in the middle pit is relatively smaller. The foundation pit was excavated to a position of 5 m, and the maximum bulge value at the bottom of the pit was 22.39 mm. When excavation was carried out to 8 m, soil uplift still occurred in the bottom of the pit and the maximum value of the uplift was 31.39 mm. In addition, the rate of soil uplift caused by excavation gradually decreases with increase in excavation depth.

4.2. Horizontal Displacement

As the excavation depth increases, soil pressure gradually increases, leading to a rise in horizontal displacement in the side wall of the foundation pit. Figure 7 shows the horizontal displacement of the foundation pit in the direction of length and width on completion of the excavation. Maximum horizontal displacement occurs along the width of the pit, the maximum value of which is 36.12 mm—0.45% of the excavation depth. The horizontal displacement of the foundation pit gradually takes on a “bulk belly” form with increase in excavation depth—a larger middle and lower part and a smaller upper part.

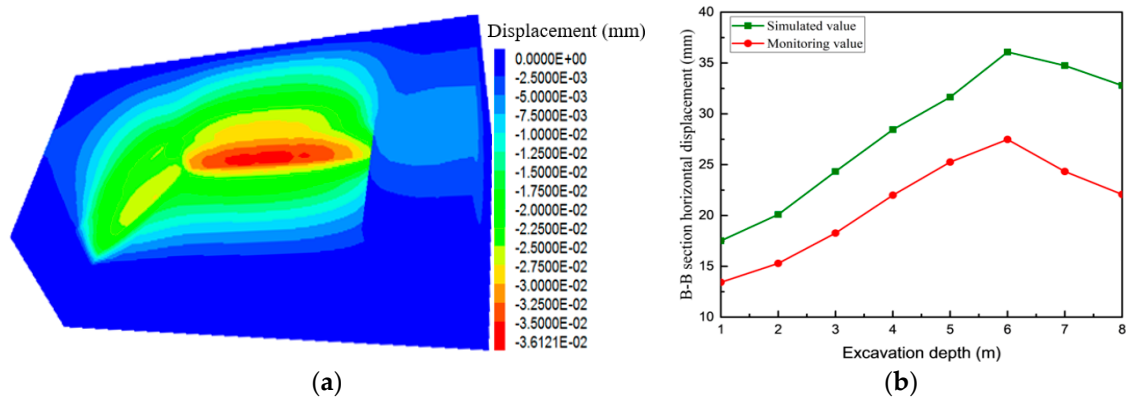


Figure 7. Horizontal displacement at different excavation depths: (a) Cloud diagram showing the horizontal displacement of soil in a foundation pit; (b) Monitoring curve showing the horizontal displacement of soil.

In order to verify the correctness and rationality of the numerical simulation results, the simulation results of the horizontal displacement of soil are compared with the measured values. As shown in Figure 7, the simulation values are basically consistent with the measured values. After the excavation, the measured horizontal displacement of soil on the side wall of the foundation pit was 27.46 mm. The simulation value has certain errors, but within an allowable range. Thus, this proves the correctness and rationality of the numerical simulation results. In addition, with increase in the horizontal displacement on the side wall of the foundation pit, its growth rate gradually decreases. The reason for this change is because when soil nails are excavated, the reinforcement effect of the upper soil is improved to a certain extent.

4.3. Axial Force of Soil Nailing

As shown in Figure 8, the distribution of the axial force is fusiform in shape. The maximum axial force gradually increases with increase in excavation depth. The axial force in the middle and lower parts of the whole supporting structure is significantly larger than that of the remaining parts, which is because earth pressure of the upper supporting structure is gradually applied to the middle and lower soil nails as the excavation progresses. In the whole construction process, the stress of the first row of soil nails is smaller, because it was constructed after complete excavation of the first layer of soil. The axial force of the first row mainly acts on the soil below the first row of soil nails, and further plays a role in restraining lateral displacement of the soil. In addition to constraints on the soil below the second row of soil nails, there also are restrictions on the first layer of soil. Similar force in each row of soil nails also occurs when downward excavation continues, until excavation in the eighth layer of soil. As the eighth row of soil nails has a relatively small displacement constraint on the soil under it, the force of the eighth row of soil nails is relatively small. Therefore, in on-site construction, reasonable arrangement in number and spacing of soil nails per row can reduce costs.

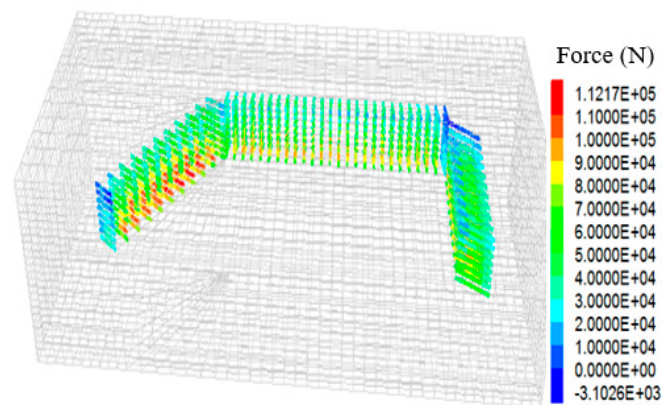


Figure 8. Horizontal displacement at excavation depths of 8 m.

4.4. Foundation Pit Stability

Figure 9 presents diagrams for shear strain rate and velocity vector. As can be seen from the figure, safety factor is 1.46. The shear plastic failure zone penetrates the bottom of the foundation pit and the ground surrounding it. A sliding surface then begins to appear in the area beyond the soil nail-reinforced region outside the pit. Therefore, the soil layer is strengthened by soil nails and forms a whole layer that has a reinforcing effect on the pit. Only overall slip of the foundation pit occurs, instead of a single side slip. Figure 9 shows that soil velocity in the sliding region is much larger than that in the surrounding soil. With the formation of a sliding zone, the sliding body begins to gradually move, causing instability in the foundation pit.

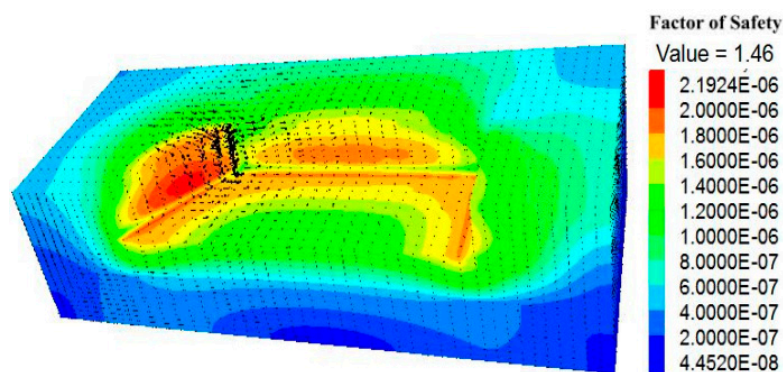


Figure 9. Shear strain rate and velocity vector diagram.

5. Deformation Characteristics

5.1. Effect of Soil Nails on Deformation

5.1.1. Inclination Angles of Soil Nails

The inclination angle of the soil nails is set to 5°, 10°, 15°, 20°, 25°, 30°, and 35° respectively. In order to adhere to the law, the excavation depth of the foundation pit was extended to 10 m. As shown in Figure 10, there is a positive correlation between inclination of soil nails and horizontal displacement at the top of the foundation pit. When the inclination increases from 30° to 35°, the horizontal displacement at the top of the slope and the maximum horizontal displacement have obvious break points. After the excavation, the main tensile strain in the soil is found to be close to the horizontal direction, and its growth rate obviously increases. Soil displacement gradually moves away from the main tensile strain as the inclination angle of the soil nail increases; bending stiffness is found to be small, and the constraint on lateral deformation is relatively small. Therefore, the horizontal

soil displacement increases with rise in inclination angle. When applying the soil nailing technique in actual engineering, it is necessary to consider the impact of the construction process. Horizontal arrangements should be avoided as far as possible, and inclination of the soil nail should be kept below 30°.

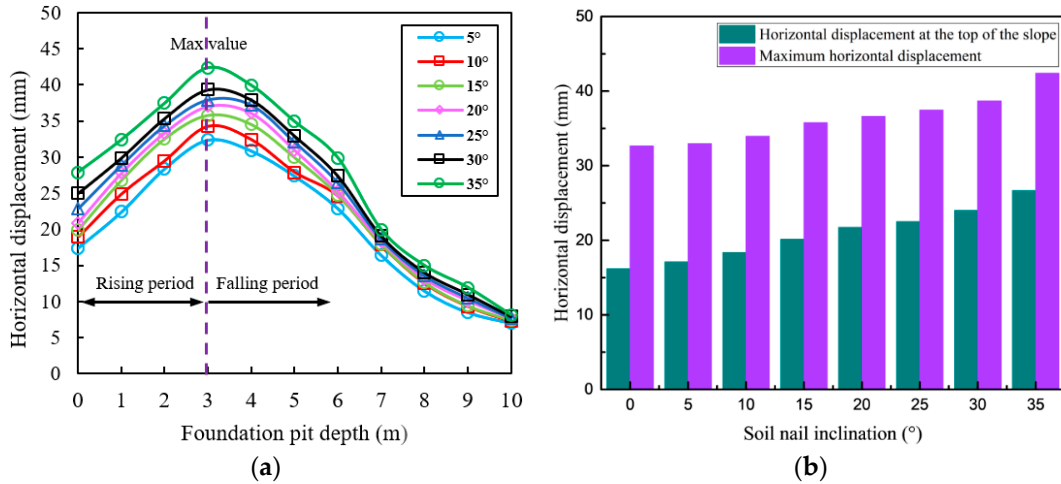


Figure 10. The effect of soil nail inclination angles on horizontal displacement: (a) The effect of soil nail inclination on horizontal displacement; (b) The effect of soil nail inclination on horizontal displacement of slope top and maximum horizontal displacement.

5.1.2. Prestressing of Soil Nails

Prestresses are applied to the second and third row of soil nails—0 kN, 10 kN, 20 kN, 30 kN, and 40 kN, respectively. The effect of prestress on deformation of the foundation pit is presented in Figure 11. The changes in horizontal displacement have nothing to do with whether prestress is applied or not; both rising and falling periods are visible. After the second and third row of soil nails are prestressed, the horizontal displacement of the foundation pit is significantly reduced. As the prestress increases, the horizontal displacement continues to decrease. When the prestress exceeds 20 kN, the effect on the horizontal deformation becomes less noticeable. The deformation of soil nails can be quickly optimized, and the supporting performance of soil nails can be brought into full play by prestressing; this results in a reduction in deformation. Actual engineering has strict requirements for prestressing of soil nails, and it is recommended that prestressing values be between 10 kN~20 kN.

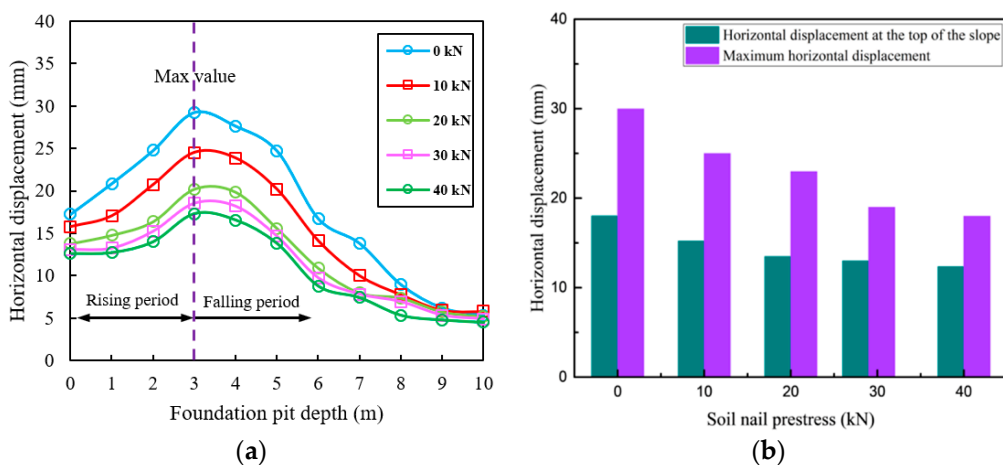


Figure 11. The effect of soil nail prestress on the horizontal displacement: (a) The effect of soil nail prestress on horizontal displacement; (b) The effect of soil nail prestress on horizontal displacement of slope top and maximum horizontal displacement.

5.2. Effect of Mixing Pile on Deformation

5.2.1. Diameter of the Mixing Pile

The stiffness of a mixing pile is related to its elastic modulus and diameter. Here, the method used to change the diameter of the mixing pile is also used to alter its stiffness. The diameter of the mixing pile is 0.5 m, 1.0 m, 1.5 m, 2.0 m, and 2.5 m. As shown in Figure 12, with increase in the diameter of the mixing pile, the horizontal displacement of the foundation pit and its deformation rate is obviously reduced. The influence of stiffness of the mixing pile on the maximum horizontal displacement of the foundation pit is greater than that of the horizontal displacement of the slope. When the diameter of the mixing pile reaches 1.5 m, the stiffness has little effect on the horizontal displacement at the slope top and maximum horizontal displacement, which is about 0.2 times the depth of the foundation pit excavation. Therefore, deformation can be controlled by increasing the diameter of the mixing pile, but with suitable values.

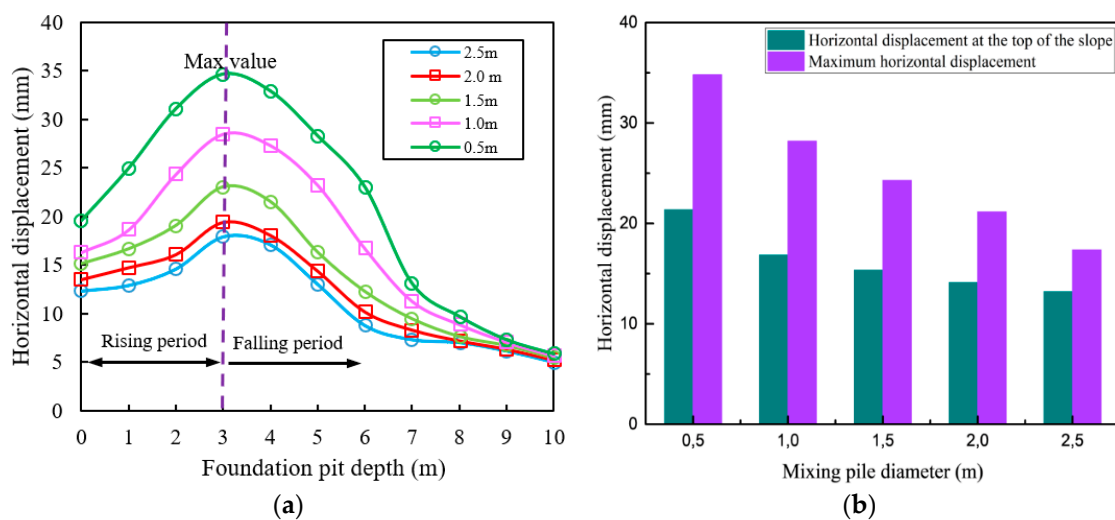


Figure 12. The effect of diameter of the mixing pile on horizontal displacement of soil: (a) The effect of soil nail diameter on horizontal displacement; (b) The effect of soil nail diameter on horizontal displacement of the slope top and maximum horizontal displacement.

5.2.2. Embedded Depth of the Mixing Pile

Figure 13 presents the effect of embedded depth of the mixing pile on the horizontal displacement. We can see that the deeper the embedded depth of the mixing pile, the smaller the horizontal displacement of the foundation pit. At embedded depth of 1 or 2 m, the horizontal displacement of the foundation pit is large. When the embedded depth of the mixing pile is more than 3 m, the horizontal displacement decreases significantly. The effect of embedded depth on the horizontal displacement is negligible. It can thus be concluded that there is a critical value for the influence of the embedded depth of the mixing pile on the horizontal displacement. When the embedded depth of the mixing pile exceeds that critical depth, the limiting effect of the mixing pile on the horizontal displacement is not significant. The excavation depth of the foundation pit in this simulation was 8 m, and the obtained critical depth of the mixing pile was about 0.4 times that value.

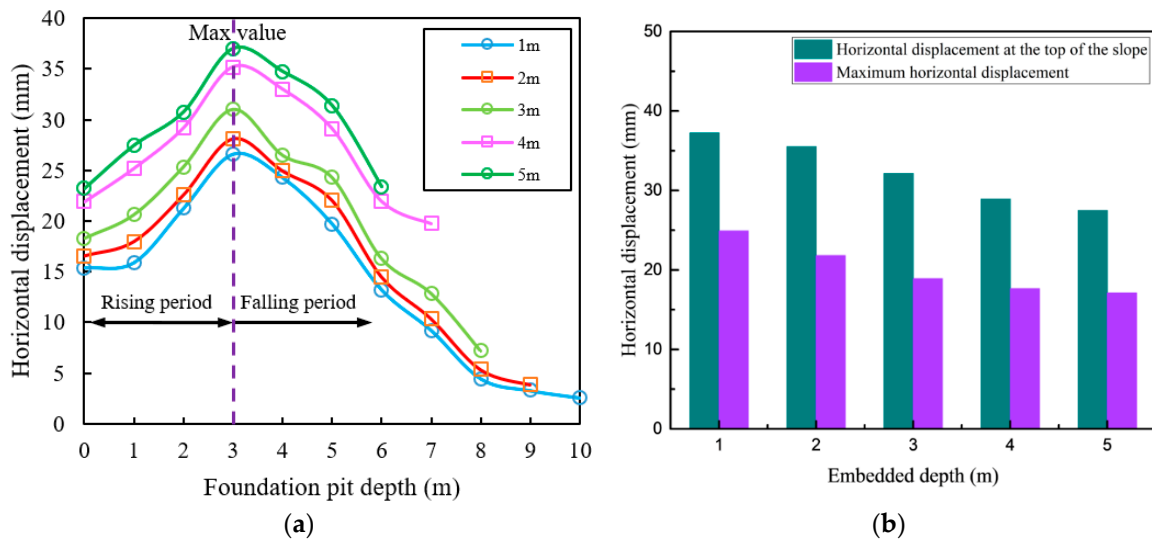


Figure 13. The effect of embedded depth of the mixing pile on horizontal displacement: (a) Effect of embedded depth of mixing pile on horizontal displacement; (b) Effect of embedded depth of mixing pile on horizontal displacement of slope top and maximum horizontal displacement.

5.2.3. Mixing Pile Position from the Excavation Surface

This section discusses a simulation analysis of mixing piles placed at 0 m, 2 m, 4 m, and 6 m from the excavation surface. As shown in Figure 14, the horizontal displacement of the foundation pit increases in relation to distance of the mixing pile from the excavation surface; however, its growth rate is not significant. The horizontal displacement at the top of the slope increases with the distance between the excavation faces of the mixing pile. When it exceeds 6 m, it has a greater influence on the displacement. As the excavation continues, the deformation of the soil gradually moves towards the common soil nail wall. Thus, when the setting position of the mixing pile is changed and its distance from the excavation surface increases, timely monitoring and control of the horizontal displacement is essential to prevent the pit slope by sliding, an activity caused by excessive deformation of the slope top.

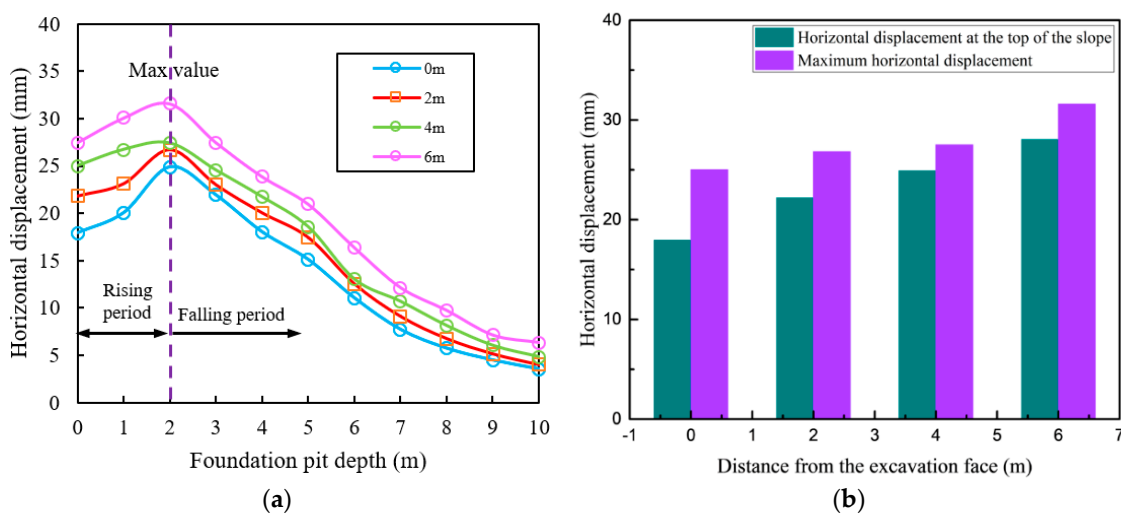


Figure 14. The effect of mixing pile position from the excavation surface on horizontal displacement: (a) Effect of the position of the mixing pile on horizontal displacement; (b) Effect of the position of the mixing pile on the horizontal displacement of the slope top and maximum horizontal displacement.

6. Conclusions

This paper employs FLAC3D to investigate the sensitivity and deformation characteristics of a symmetrical foundation pit supported by composite soil nailing in muddy soft soil. The main conclusions are as follows:

(1) The orthogonal experimental shows that the degree of the control indicators affecting the stability of the foundation pit is $h > E > C > F > H$, which indicates that excavation depth h of the foundation pit has the greatest influence on stability.

(2) Composite soil nail support has poor control on settlement outside the foundation pit. The uplift of soil inside the foundation pit mainly occurs at the bottom, presenting a tendency to affect small areas in the middle and large areas surrounding the pit.

(3) The horizontal displacement of soil on the side wall gradually changes to a “bulk belly” shape as excavation depth increases. Maximum horizontal displacement occurs along the width of the pit. In addition, with excavation of the foundation pit, the growth rate of horizontal displacement gradually decreases.

(4) The inclination and spacing of the soil nails as well as distance of the mixing pile from the excavation surface are positively correlated with horizontal displacement of the foundation pit. However, the relationship between the diameter and embedded depth of the mixing pile and horizontal displacement is negatively correlated.

(5) The inclination and spacing of soil nails, diameter and buried depth of mixing piles, and the depth of inlays have their own critical values for stability of the foundation pit. The determination method and corresponding results are discussed in this paper. Specifically, when it is larger than the critical value, the limiting effect of the composite soil nailing structure is not obvious. Therefore, it is necessary to strictly determine support parameters that meet economic and security requirements.

Author Contributions: All the authors contributed to publishing of this paper. Conceptualization, H.L.; methodology, W.H.; software, Z.S. and G.L.; validation, H.L. and C.L.; formal analysis, W.H.; investigation, X.W.; writing—original draft preparation, Z.S.; writing—review and editing, W.H. and G.L.; supervision, H.L.; funding acquisition, H.L. All authors have read and agreed to the published version of the manuscript.

Funding: This research and the APC were both funded by the Shandong Provincial Natural Science Foundation, China (Grant No. ZR2019BEE065).

Conflicts of Interest: The authors declare no conflicts of interest.

References

1. Cheng, Y.M.; Au, S.K.; Yeung, A.T. Laboratory and Field Evaluation of Several Types of Soil Nails for Different Geological Conditions. *Can. Geotech. J.* **2016**, *53*, 634–645. [[CrossRef](#)]
2. Peng, W.; Xie, Y.; Xu, S.; Wang, Y.; Qian, H. Experimental study on working behavior of prestressed anchor composite soil nailing wall. *J. Cent. South Univ. (Nat. Sci. Ed.)* **2015**, *46*, 1468–1474.
3. Qin, S.; Chen, H.; Zhang, M. Numerical Simulation Analysis of Deformation and Failure of Soil Nail Support Structure by Finite Element Method. *Prospect. Eng. Geotech. Eng.* **2005**, *01*, 102–105.
4. Qin, S.; Jia, H.; Ma, P. Numerical analysis of deformation and failure of prestressed soil nailed retaining structures. *China Rock Soil Mech.* **2005**, *27*, 1356–1362.
5. Zhu, H.-H.; Yin, J.-H.; Yeung, A.T.; Jin, W. Field Pullout Testing and Performance Evaluation of GFRP Soil Nails. *J. Geotech. Geoenviron. Eng.* **2011**, *137*, 633–642. [[CrossRef](#)]
6. Jamsawang, P.; Yoobanpot, N.; Thanasisathit, N.; Voottipruex, P.; Jongpradist, P. Three-dimensional numerical analysis of a DCM column-supported highway embankment. *Comput. Geotech.* **2016**, *72*, 42–56. [[CrossRef](#)]
7. Oliveira, P.J.V.; Pinheiro, J.o.L.P.; Correia, A.A.S. Numerical analysis of an embankment built on soft soil reinforced with deep mixing columns: Parametric study. *Comput. Geotech.* **2011**, *38*, 566–576. [[CrossRef](#)]
8. Yapage, N.N.S.; Liyanapathirana, D.S.; Kelly, R.B.; Poulos, H.G.; Leo, C.J. Numerical Modeling of an Embankment over Soft Ground Improved with Deep Cement Mixed Columns: Case History. *J. Geotech. Geoenviron. Eng.* **2014**, *140*, 04014062. [[CrossRef](#)]

9. Lin, G. Finite Element Analysis of Composite Soil Nailing Support System for Cement-Soil Mixing Piles. Ph.D. Thesis, South China University of Technology, Guangzhou, China, 2015.
10. Huang, J.H. Finite Element Analysis of Composite Soil-Nail Retaining Structure in Foundation Pit Engineering. *Appl. Mech. Mater.* **2012**, *204–208*, 163–167. [[CrossRef](#)]
11. Zeng, X. Experimental Study on Similar Model of Soil Nail Supporting Soft Soil Side Wall (Slope) Mechanism. *Chin. J. Rock Mech. Eng.* **2000**, *19*, 534–538.
12. Yu, J.; Zou, Y. Model test study of soil nailing support structure. *Soil Eng. Found.* **1998**, *12*, 14–19.
13. Zhang, J.; Zhang, Y.; Pu, J. Research on Centrifugal Model Test of Soil Nailing Support. *Chin. J. Civ. Eng.* **2009**, *42*. [[CrossRef](#)]
14. Guo, H.; Song, E.X.; Chen, Z. Influence surface of soil nailing support excavation and its application in soil nail force calculation. *China Eng. Mech.* **2007**, *24*.
15. Zeng, Y. The Analys of Stability of Composite Soil Nail. *Appl. Mech. Mater.* **2014**, *580*, 503–508. [[CrossRef](#)]
16. Xu, S. Numerical Simulation of Composite Soil-Nailed Foundation Pits Supported by Cement-Soil Mixing Piles. Ph.D. Thesis, Taiyuan University of Technology, Taiyuan, China, 2011.
17. Lin, Z. Deformation Analysis of Composite Soil Nailed Support Structure of Mixing Pile. Ph.D. Thesis, Guangzhou University, Guangzhou, China, 2013.
18. Huang, J.H.; Song, G.; Song, E.X. Optimization Simulations of Support System by Composite Soil-Nail Retaining Structure. *Appl. Mech. Mater.* **2012**, *166–169*, 863–868. [[CrossRef](#)]
19. Hui, L.; Zhao, P.; Li, G.; Li, G. Time-effect analysis of deep foundation pit excavation and support in soft clay soil areas. In Proceedings of the International Conference on Remote Sensing, Environment and Transportation Engineering, Nanjing, China, 24–26 June 2011.
20. Yu, T.X. Support Design and Monitoring Analysis of Foundation Pit Adjacent to High Speed Railway in Soft Soil Area. 2015. Available online: https://www.researchgate.net/publication/290519678_Support_design_and_monitoring_analysis_of_foundation_pit_adjacent_to_high_speed_railway_in_soft_soil_area#references (accessed on 1 January 2020).
21. Zeng, X.M.; Huang, J.S.; Wang, Z.M.; Song, H.M. Manual for Design and Construction of Soil Nailing Support. Master's Thesis, China Building Industry Press, Beijing, China, 2000.



© 2020 by the authors. Licensee MDPI, Basel, Switzerland. This article is an open access article distributed under the terms and conditions of the Creative Commons Attribution (CC BY) license (<http://creativecommons.org/licenses/by/4.0/>).